The Relationship between Storm Motion, Vertical Wind Shear, and Convective Asymmetries in Tropical Cyclones

Kristen L. Corbosiero and John Molinari

Department of Earth and Atmospheric Sciences, The University at Albany, State University of New York, Albany, New York

ABSTRACT

The influence of the direction of storm motion on the azimuthal distribution of electrified convection in 35 Atlantic basin tropical cyclones from 1985 to 1999 was examined using data from the National Lightning Detection Network. In the inner 100 km, flashes most often occurred in the front half of storms, with a preference for the right-front quadrant. In the outer rainbands ($r = 100$–300 km), flashes occurred predominantly to the right of motion, although the maximum remained in the right-front quadrant. The results are shown to be consistent with previous studies of asymmetries in rainfall, radar reflectivity, and vertical motion with respect to tropical cyclone motion. The motion effect has been attributed to the influence of asymmetric friction in the tropical cyclone boundary layer.

The authors previously found a strong signature in the azimuthal distribution of lightning with respect to vertical wind shear. Because both effects show clearly, vertical wind shear and storm motion must themselves be systematically related. It was found that more than three-quarters of 12-hourly periods contained a storm motion vector that was left of (i.e., counterclockwise from) the shear vector. These results support the importance of a downshear shift in the upper anticyclone, which produces motion left of shear for all directions of shear. The results are further broken down by direction of shear, and it is shown that the beta effect also plays a significant role in the relationship between motion and vertical wind shear. These results also suggest that substantial downshear tilt of the *cyclonic* part of the tropical cyclone vortex is uncommon, because that alone produces motion right of shear.

The relative importance of asymmetric friction and vertical wind shear on the azimuthal asymmetry of convection was determined by examining circumstances in which the two effects would place maximum lightning in different quadrants. Without exception, the influence of vertical wind shear dominated the distribution. Although asymmetric friction creates vertical motion asymmetries at the top of the boundary layer, these apparently do not produce deep convection if vertical wind shear–induced circulations oppose them.

1. Introduction

Corbosiero and Molinari (2002) found a strong correlation between the azimuthal distribution of electrified convection in tropical cyclones and the direction of the 850–200-hPa vertical wind shear in the environment. For magnitudes of shear greater than 5 m s^{-1}, more than 90% of flashes occurred downshear of the center. A preference for downshear left was seen in the inner core region, while a strong preference for the downshear right quadrant was found for the outer bands.

In the current paper, the effects of storm motion on convective asymmetries in tropical cyclones, as measured by lightning frequency and distribution, will be evaluated. All named storms in the Atlantic basin that moved within range of the National Lightning Detection Network (NLDN) will be studied, both over ocean and over land, as long as they remained classified as tropical systems by the National Hurricane Center (NHC). The results will be compared to those predicted by theory and numerical modeling, and to previous observations using radar reflectivity, precipitation, and vertical motion. As shown by Shapiro (1983), the motion effect arises from asymmetric frictional forcing in the boundary layer.

Since both vertical wind shear and asymmetric friction are continuously acting to create the observed asymmetries in convection, it follows to ask which of the effects plays a greater role in determining the overall distribution of lightning. It is possible that either signal may simply be an artifact of the other if vertical wind shear and storm motion have a systematic relationship. These possibilities are examined in the second half of the paper.

Corresponding author address: Kristen L. Corbosiero, Department of Earth and Atmospheric Sciences, The University at Albany, SUNY, 1400 Washington Avenue, Albany, NY 12222.
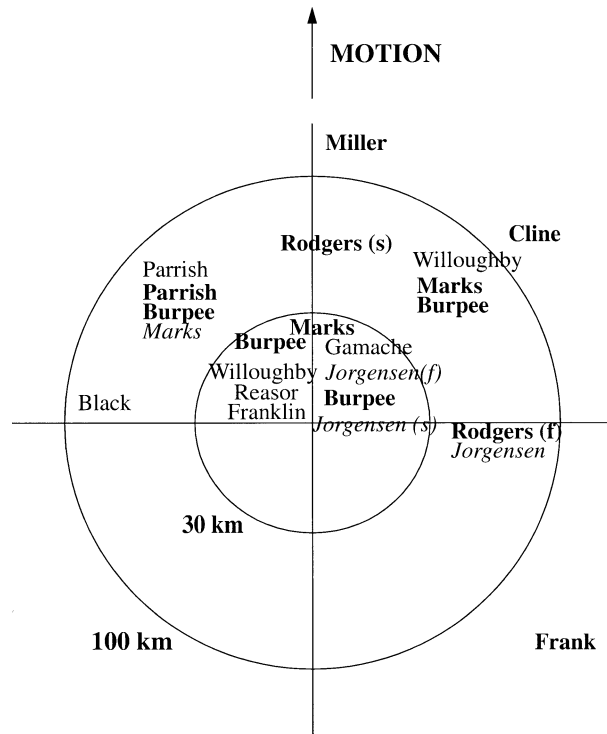E-mail: kristen@atmos.albany.edu

FIG. 1. Distribution of the results of the observational studies reviewed in the text. Each name represents the lead author of the paper and is positioned around the storm in the motion-rotated quadrant of the maxima of the quantity described. Bold names refer to precipitation maxima, italics are vertical motion maxima, and plain text are reflectivity maxima. The symbols f and s refer to fast and slow storm motion, respectively.

2. Review of motion effects on tropical cyclones

a. Observational studies

Figure 1 summarizes the results of the major studies that have investigated asymmetries in tropical cyclones with respect to storm motion. The location of the maximum of the quantity studied (precipitation, reflectivity, upward vertical motion, etc.) in each paper is plotted by the name of the first author and appears in the motion-rotated (the motion vector points due north) quadrant and radial ring of the major asymmetry described. Papers focusing on maxima in precipitation, vertical motion, and radar reflectivity are plotted in bold text, italics, and plain text, respectively.

Terminology in this paper will be as follows: in the direction of the motion vector will be referred to as front, and in the direction of the vertical wind shear vector will be referred to as downshear. The opposite directions are rear and upshear, respectively.

In the eyewall ($r \leq 30$ km), Jorgensen et al. (1985) found maximum upward mass transport in slow-moving (<5 m s^{-1}) storms occurred to the right of motion, with equal amounts front and rear, while fast-moving ($\sim$10 m s^{-1}) storms showed a slight preference for the right-front quadrant. The maximum precipitation in the eyewall was found within 90° of the direction of motion, in the left-front quadrant of Hurricane Allen (1980), the right-front quadrant of Hurricane Elena (1985), and directly in front of Hurricane Alicia (1983) by Marks (1985) and Burpee and Black (1989), respectively. Willoughby et al. (1984), Franklin et al. (1993), and Reasor et al. (2000) examined the patterns of reflectivity in the eyewalls of Hurricanes David (1979) and Gert (1981), Hurricane Gloria (1985), and Hurricane Olivia (1994). They found a consistent left-of-motion maximum in radar reflectivity values, except for one time period of Olivia (1994) in which the maximum shifted into the right-front quadrant (Gamache et al. 1997).

The largest number of studies has examined the distribution of precipitation in the inner rainband region (30 km $< r \leq 100$ km) and the results are scattered. Jorgensen et al. (1985) found that updraft cores were concentrated to the right of motion with no notable differences between slow and fast movers, while Marks et al. (1992) found maximum upward vertical velocities in the left-front quadrant of Hurricane Norbert (1984). Parrish et al. (1982) and Burpee and Black (1989) found left-front quadrant maxima in precipitation in Hurricanes Frederick (1979) and Alicia (1983), while Marks's (1985) study of Allen (1980) and Burpee and Black's (1989) examination of Elena (1985) yielded maximum precipitation in the right-front quadrant. Rodgers et al. (1994) examined 18 named North Atlantic tropical cyclones and found the heaviest (>5 mm h^{-1}) rain in the front half of slow-moving (<4.1 m s^{-1}) storms, and to the right of fast-moving (>7.7 m s^{-1}) storms. Parrish et al. (1982) and Black et al. (1997) found reflectivity maxima in the left-front quadrant, while Willoughby et al. (1984) found the inner rainbands to curve cyclonically outward from directly in front of Hurricanes David (1979) and Gert (1981) to the right-front quadrant with increasing radius.

Only three studies have investigated asymmetries in precipitation at large radii ($r > 100$ km). Cline (1926) and Miller (1958) found that rainfall rates were significantly higher ahead of the storms than behind and slightly higher to the right of the tracks, while Frank (1977) found a nearly symmetric distribution of precipitation with a slight preference for the right-rear quadrant.

Although these earlier individual studies make use of a number of variables (precipitation, radar reflectivity, and vertical motion) to define convective asymmetries, and show varying results, a reasonably clear influence of storm motion appears in Fig. 1. A strong preference occurs for maximum convection in the front quadrants in the core and inner band regions, with a slight preference for right of motion as well. When radii outside 100 km are considered, maximum values of precipitation were observed to the right of motion, with a preference for the right-front quadrant. The maximum upward vertical motion, reflectivity or rainfall never occurs in the left-rear quadrant.

b. Numerical studies

Among the studies that have sought to model the effects of storm motion on the azimuthal distribution of convection in tropical cyclones, the most notable is the work of Shapiro (1983). A slab boundary layer model was used to investigate the effects of translation on the boundary layer winds, friction, and distribution of convergence within a hurricane-like vortex. For slow-moving (<5 m s^{-1}) storms, maximum frictional convergence was observed in a broad arc ahead of the storm center. When the translational speed of the vortex was increased to 10 m s^{-1}, the convergence rotated clockwise and became concentrated in the right-front quadrant. For radii greater than 100 km, the maximum inflow angle was found to be in the right rear of a modeled vortex moving at 10 m s^{-1}.

This azimuthal distribution of convergence with respect to motion can be understood in terms of the asymmetric friction within the storm. The addition of the basic current moving the vortex to the cyclonic winds of the storm produces the strongest winds to the right of the direction of motion. The frictional force is roughly proportional to the square of the wind speed, and thus an increased frictional force is observed to the right of the vortex. The maximum inflow angle and convergence are found in front and to the right of the translating vortex (Shapiro 1983). This influence, clearly identified in idealized models, will be referred to in the remainder of the paper as the storm motion effect.

The results presented by Shapiro (1983) are consistent with the more recent studies of Bender (1997) and Frank and Ritchie (1999). Both found frictional effects produce a broad arc of convergence ahead of and to the right of storm motion. The results of these idealized numerical modeling studies correspond well with the observations in Fig. 1.

3. Storm motion

A complete discussion of the data and methodology for this study is given by Corbosiero and Molinari (2002) and thus only a summary of the pertinent information will be given here. All named tropical cyclones from 1985–99 that were over land or came within 400 km of the United States coastline (the nominal limit of the NLDN; see Molinari et al. 1999) were considered for this study. Since the distribution of lightning with respect to storm motion is the focus of this work, the total number of hours a storm was within range of the NLDN was divided into 12-hourly periods, each with its own storm motion vector calculated from the best track center positions. This partitioning of the data yielded 303 time periods from 35 tropical cyclones. Each time period will be treated as an individual data point with its own unique storm motion vector and lightning distribution.
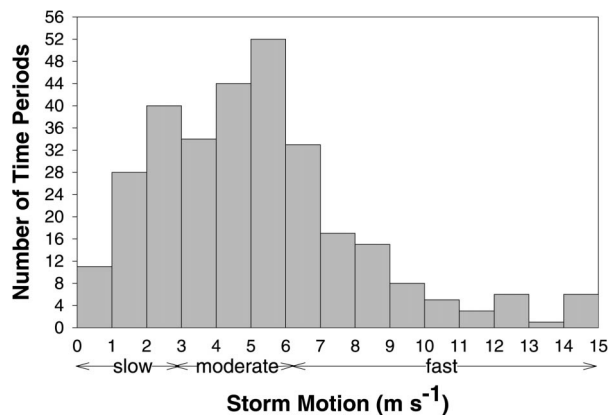

FIG. 2. Distribution of the magnitude of storm motion (m s^{-1}) for all 303 12-h time periods. The three speed categories used are slow: <3 m s^{-1}; moderate: 3–6 m s^{-1}; and fast: >6 m s^{-1}.

a. Distribution of storm motion

A storm motion vector was calculated every 12 h using a 12-h centered differencing scheme. The distribution of the speed of motion for all 303 12-h time periods is shown in Fig. 2. The curve is a rough gamma distribution with a quick rise to the peak in the distribution between 5 and 6 m s^{-1} and a slow decrease in the number of cases at higher speeds.

The average speed over all time periods in this study was 5.2 m s^{-1}. This is on par with Franklin et al. (1996), who cite a mean motion of 6 m s^{-1}, and a range of 2 to 14 m s^{-1}, in their dropwindsonde study of 10 tropical storms from 1982 to 1992. Although they give no absolute counts in each category, Fiorino and Elsberry (1989) use greater than 15 kt (7.7 m s^{-1}) for fast and less than 8 kt (4.1 m s^{-1}) for slow-moving storms, which suggests a mean motion in the 5–6 m s^{-1} range. Chan and Gray (1982) also divide Atlantic tropical cyclones into fast and slow motion categories, with 4 m s^{-1} as a dividing line.

Using these studies as a guide, the motion was broken into three speed categories to quantify the effect of the magnitude of the motion on the distribution of flashes in the cases studied. Slow motion was defined as a speed below 3 m s^{-1}, moderate motion between 3 and 6 m s^{-1}, and fast motion greater than 6 m s^{-1}. This breakdown of the data gives 79 slow, 130 moderate, and 94 fast time periods. All motion effects will be discussed in this framework in the remainder of this study.

Following Corbosiero and Molinari (2002), the area around each storm was divided into two regions: the inner 100 km, hereafter referred to as the inner core, and the annulus encompassed by the 100–300-km radii, referred to as the outer band region.

In both the inner core and outer band regions, a large range of flash counts occurred over 12-h periods, from zero to several thousand. Because the azimuthal distribution of flashes is not meaningful for low flash counts, a lower-limit flash criterion was formulated to restrict

the number of time periods examined. Minimum counts of 50 and 400 flashes per time period were chosen for the inner core and outer band regions, respectively, following Corbosiero and Molinari (2002). This value was chosen to maximize the number of time periods while excluding those periods in which flashes were too few for a meaningful estimate of the quadrant of maximum lightning activity. The minimum values correspond to a flash-rate density of 16 flashes per $(100 \text{ km})^2$ per 12 h in both regions.

When the inner core flash minimum is applied to each 12-h time period, 44% of the slow, 37% of the moderate, and only 24% of the fast-moving time periods survive. The resulting number of time periods in the inner core region is 106, with 35 slow, 48 moderate, and 23 fast. From the original 35 tropical cyclones, 28 contain at least one time period with the inner core flash count exceeding the minimum. In the outer band region, 67% of the slow, 50% of the moderate, and 35% of the fast-moving time periods meet the flash minimum. The resulting number of time periods in the outer band region was 154, with 53 slow, 68 moderate, and 33 fast, coming from 30 of the original 35 tropical cyclones studied.

As is apparent from these numbers, the percentage of time periods that exceeded the minimum flash count decreased as the speed of motion of the tropical cyclones increased. The reason for this behavior is yet unknown and remains an issue for future studies.

b. Storm motion influences on lightning distribution

In order to evaluate the effect of storm motion on the distribution of lightning, the flashes in each 12-h time period were rotated around the storm center so that the motion vector for the period was pointing due north. This rotation was done separately for each of the inner core and outer band region time periods that met the minimum flash criteria. The area around each storm was divided into four quadrants with respect to storm motion, right and left front, and right and left rear. The quadrant with the highest number of flashes was then determined.

Figure 3 shows for the inner core region the number of times the flash count was highest in each motion-rotated quadrant for all time periods meeting the flash criterion. Separate boxes for each category of motion (slow, moderate, and fast) are given as well as a sum over all cases. The upper two squares of each box represent the front quadrants.

Across all speeds of motion, the highest flash counts in the inner core are most commonly found in the right-front quadrant. Seventy-one percent of the 12-h periods have their highest flash counts in the two front quadrants of the storm and 62% in the two right quadrants, which yields the maximum of 42% in the right-front quadrant. The separate quadrant plots for each of the categories of motion are notably similar to the overall quadrant plot and to each other with one exception: there is a
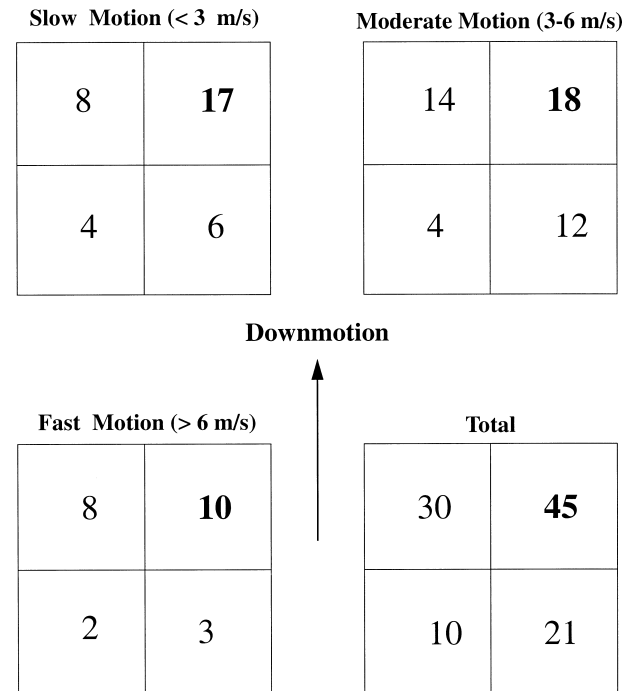

FIG. 3. Quadrant plots showing the number of times the flash count was highest in the inner core per motion-rotated quadrant for slow, moderate, and fast motion time periods. The center of each box represents the storm center, and flash locations have been rotated such that the storm motion vector points due north. Only time periods meeting the minimum flash criterion (see text) are included.

slight shift of the preferred region for lightning as the forward motion increases. The shift is from the quadrants to the right of motion to the front quadrants. This counterclockwise shift is in agreement with the vertical motion observations of Jorgensen et al. (1985), but disagrees with the clockwise shift in maximum convergence modeled by Shapiro (1983) and rainfall maxima noted by Rodgers et al. (1994). Despite this minor discrepancy, the results shown in Fig. 3 correspond well with the observed asymmetries noted in Fig. 1. The maximum number of flashes in the inner core most often occurs in the front quadrants, with a slight preference for the right front, and a minimum of activity in the left-rear quadrant.

Figure 4 shows the quadrant plot described previously for the outer band region. Once again the moderate and fast motion time periods show their highest flash counts in the right-front quadrant. The slow motion time periods, however, show nearly equal numbers of time periods in the right-front and right-rear quadrants. The quadrant plot summed over all speeds of motion shows a right-front maximum and a strong left to right asymmetry, with 76% of the highest flash counts appearing to the right of the motion vector.

The lightning asymmetries shown in Fig. 4 are similar to the few studies shown in Fig. 1 that looked at asymmetries outside the 100-km radius, in which maxima

Slow Motion (< 3 m/s)

7	20
5	**21**

Moderate Motion (3-6 m/s)

6	**32**
12	18

Downmotion ↑

Fast Motion (> 6 m/s)

3	**16**
4	10

Total

16	**68**
21	49

FIG. 4. Same as in Fig. 3 except for the outer rainband time periods.

were always right of motion with a preference for the right-front quadrant.

4. Relationships between vertical wind shear and storm motion

It was shown earlier that the preferential quadrant for lightning strikes was in the right-front quadrant with respect to storm motion for both the inner core and outer rainband regions of tropical cyclones. Corbosiero and Molinari (2002) showed that the preferential quadrant for lightning with respect to the 850–200-hPa vertical wind shear vector was the downshear left quadrant in the inner core and the downshear right quadrant in the outer bands. Since it has been shown that the distribution of lightning in tropical cyclones relates systematically to both vertical wind shear and storm motion, it follows that vertical shear and motion must themselves be related. That relationship will be investigated in this section, both from the literature and the data in this study. Once that relationship has been established, we will then consider examples to see whether the vertical wind shear or storm motion effects on convective asymmetries are greatest.

To explore the relationship between the direction of vertical wind shear and storm motion vectors in each 12-h period, the angle from the vertical shear vector counterclockwise to the motion vector was determined. For instance, if storm motion is south to north and the shear is from the west, the relevant angle is 90°. If, for the same motion, the vertical shear were from the east, the relevant angle would be 270°. The angle will also

be referred to as left of the shear vector, meaning left when facing in the direction of the vertical wind shear.

a. Previous studies

Studies by Marks et al. (1992), Franklin et al. (1993), and Gamache et al. (1997) that have mapped the three-dimensional wind fields of specific tropical cyclones have provided some limited observational information on the relationship between vertical wind shear and storm motion in tropical cyclones. Marks et al. (1992) found the shear and motion vectors to be in the same direction, both towards the northwest, in Hurricane Norbert (1984). Franklin et al. (1993) found the storm motion vector to be ~90° to the left of (counterclockwise from) the vertical wind shear in Hurricane Gloria (1985), which was moving towards the northwest in an environment with southwesterly shear. In Hurricane Olivia (1994), however, much larger separations were observed between the shear and motion vectors. Gamache et al. (1997) found the storm motion vector to be ~338° and 113° to the left of the vertical wind shear for two days of observations. In the first time period, the shear was easterly as the storm traveled towards the west-northwest, while the next day Hurricane Olivia (1994) moved towards the north in an environment of west-northwesterly shear. Thus no consistent relationship between vertical wind shear and storm motion is apparent from the small number of observations.

Numerical modeling studies of the influence of vertical wind shear on storm motion have looked at two main effects, nicely reviewed by Dengler and Reeder (1997). The first involves the interaction of the upper- and lower-level potential vorticity (PV) anomalies in a tilted vortex. As first modeled by Wu and Emanuel (1993), an initially upright hurricane-strength vortex is exposed to vertical wind shear, tilting the vortex in the downshear direction. The downward penetration of the upper-level PV anomaly interacts with the lower vortex to induce storm motion that is to the left of the wind shear vector if the upper layer is modeled as a negative (anticyclonic) anomaly (Wu and Emanuel 1993), and to the right if the upper PV anomaly is a positive (cyclonic) anomaly (Flatau et al. 1994; Wang and Holland 1996). Thus, in westerly (easterly) shear, a vortex with an upper-level anticyclonic PV anomaly would propagate towards the north (south) under this effect, always to the left of the local shear vector. Observational evidence for the downshear shift of the outflow anticyclone has been shown by Molinari et al. (1995, 1998) and Wu and Emanuel (1995a,b).

The second effect, first described by Shapiro (1992), involves the PV gradient in the environment associated with an upper-level jet. As explained by Flatau et al. (1994), in the absence of a planetary vorticity gradient (f plane) and assuming horizontally uniform geostrophic flow, the meridional gradient of PV is determined solely by the second derivative of the zonal wind:
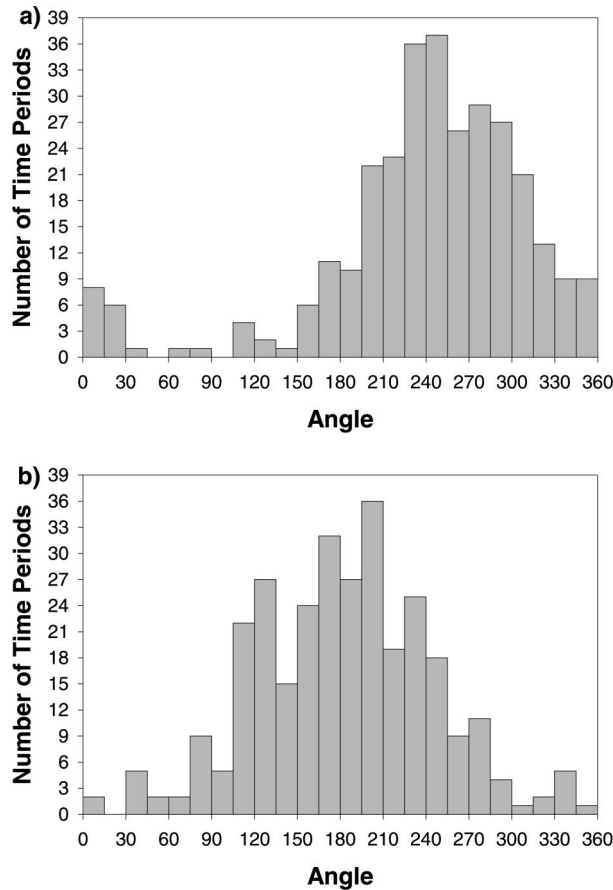
a)

b)

FIG. 5. Distributions of the meteorological direction of the (a) vertical wind shear and (b) storm motion in all 303 12-h time periods examined.

$$\partial q/\partial y \sim f\partial/\partial z(\partial\Theta/\partial y) \sim -\partial^2 u_g/\partial z^2$$

Thus, linear variations of the zonal wind with height are not associated with a meridional PV gradient, and this second effect on motion vanishes when shear is constant in the vertical. However, when westerly shear increases with height there must be an accompanying equatorward gradient in PV. The cyclonic circulation of the hurricane vortex acting on this gradient will advect low PV air southward on the west side of the center, and high PV air northward on the east side of the vortex (Shapiro 1992). This advection induces a negative PV anomaly southwest of the center and a positive PV anomaly to the northeast. The circulation around these anomalies produces northwesterly flow across the vortex and the vortex moves towards the southeast (Dengler and Reeder 1997), 45° to the right of the shear vector.

Studies that have modeled both effects and their relative influence on the motion have come up with opposing conclusions. Shapiro (1992) concluded that the motion due to the tilting vortex was secondary to the PV gradient in the environment as his modeled vortices all moved to the right of the shear. This agrees with the findings of Flatau et al. (1994) who found motion to
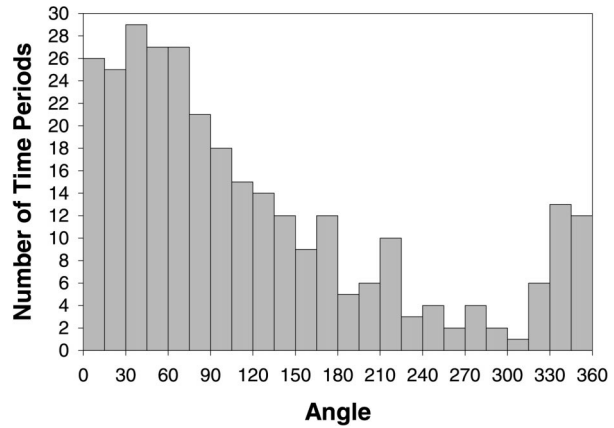

FIG. 6. Distribution of the angle between the vertical wind shear and storm motion vectors for all 303 12-h periods, measured counterclockwise from the vertical shear to the motion vector.

the left of a linear shear vector (tilt of anticyclone only), and to the right of a nonlinear shear vector. Dengler and Reeder (1997), however, found that vortices moved to the left of shear during the first 36 h of their integration, but then curved around to move right of shear as the upper-level anticyclone was carried too far away (>1500 km) from the lower center to influence its motion. They concluded that the tilt was the dominant factor in determining the motion as the vortices moved to the northeast when under both effects.

Because of the differing model results presented above and the absence of a large-scale observational study of the relationship between the angle of tropical storm motion and environmental wind shear, the datasets compiled for this study will be used to address this question. In the remainder of this section, average shear and motion vectors calculated for the dataset as a whole will be discussed. The angle between shear and motion for each time period is also calculated and compared to the results of the studies reviewed earlier.

b. Angle between the shear and motion vectors

Figures 5a and 5b show the distributions of the directions of vertical wind shear and storm motion for all 303 12-h time periods. Both distributions are roughly bell curves with an average shear vector from the west-southwest (255°) and an average motion vector that is from the south-southwest (188°).

The distribution of the angle between shear and motion vectors (measured counterclockwise from the shear to motion vector) for all time periods is shown in Fig. 6. The most common angles of separation are between 0° and 75°, with a maximum between 30° and 45°. Fifty-one percent of the time periods have a motion vector between 0° and 90° left of shear. This fits with the typical west or southwest shear and motion towards the north to northeast of tropical cyclones approaching the United States. The number of cases rapidly decreases when the
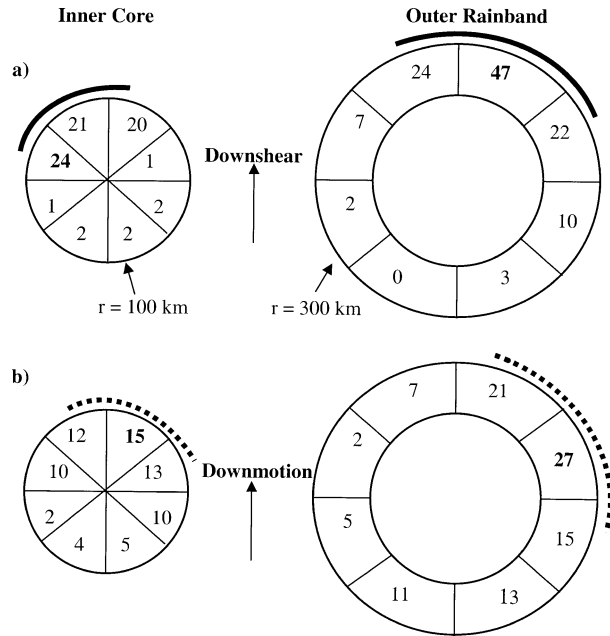
FIG. 7. The number of times the flash count was highest in the inner core and outer rainband regions of (a) the time periods with a vertical wind shear of ≥ 5 m s^{-1} and (b) the time periods with a storm motion of ≥ 3 m s^{-1}. Based on these distributions, the locations of expected maxima of lightning are shown with respect to vertical wind shear (solid line) and storm motion (dashed line).
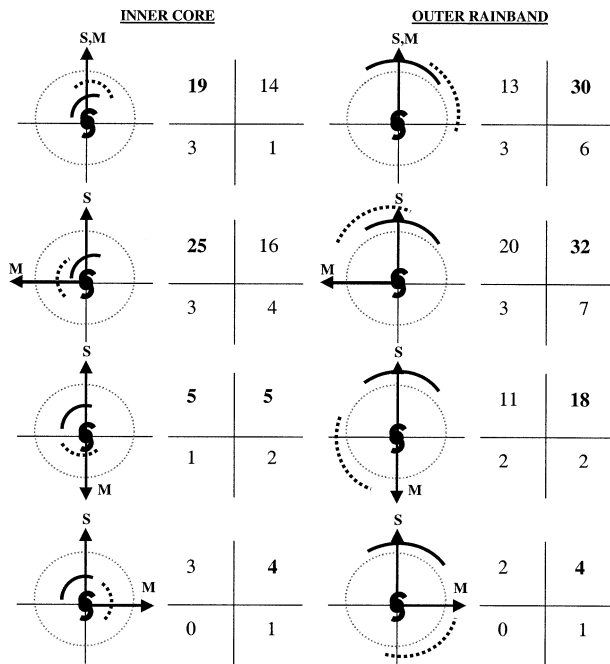

FIG. 8. Schematic representation of expected lightning maxima for different angles of separation between shear and motion (0°, 90°, 180° and 270°, all ±45°) for the inner core and outer rainband regions. The shear and motion vectors are drawn in heavy black arrows and labeled S and M, respectively; the dotted gray line is the 100-km radius; the solid black curves are the expected lightning maxima from vertical wind shear and the dashed lines from storm motion, following Fig. 7.

motion vector is more than 90° left of the shear vector, until the minimum in the distribution around 300° (i.e., the motion vector is 60° clockwise of the vertical shear). The number of cases then increases again as the angle returns to 0°.

The distribution in Fig. 6 will be divided into two halves: those time periods with a left-of-shear motion vector (0°–180° angle separation) and those to the right (180°–360° angle separation). A substantial number, 235 of the 303 time periods (78%), have a left-of-shear motion vector. This result supports the theory of a broad upper-level anticyclone advected downshear of the low-level center and inducing motion to the left of the shear as discussed by Wu and Emanuel (1993) and Dengler and Reeder (1997).

A further examination of these results appears in the discussion (section 6).

5. The relative influence of the vertical wind shear and storm motion effects on convective distribution

To compare the relative influence of vertical wind shear and storm motion on the distribution of lightning in tropical cyclones, the shear and motion signatures must first be clearly defined. Figures 7a and 7b show the number of times the flash count was highest, per octant, in both the inner core and outer rainband regions of the time periods with a vertical wind shear of ≥ 5 m s^{-1} (the medium- and strong-shear cases from Corbosiero and Molinari 2002) and the time periods with a storm motion of ≥ 3 m s^{-1} (the moderate and fast motion cases defined above). Figure 7a shows that the greatest lightning activity in the core occurred directly downshear and downshear left of the center. In the outer band region, the highest flash counts were observed to be downshear and downshear right of the center. Of note is the very sharp decrease in the number of time periods per octant away from downshear. The heavy black lines marked in Fig. 7a represent the octants in which the highest flash counts were most frequently observed. These octants will be referred to as the preferred octants or expected maxima in lightning with respect to vertical wind shear.

Figure 7b shows a preference for inner core flashes in the three octants comprising the area in front and to the right of storm motion. In the outer band region, the highest flash counts are most often observed clockwise of the inner core maximum, in the right-front quadrant and extending to the right rear. The octants of preferred lightning flashes with respect to motion in both the core and outer band regions are marked with heavy dashed lines in Fig. 7b.

Putting together the key results of Figs. 7a and b, a schematic drawing of the relative placement of the lightning asymmetries found with respect to both storm motion and vertical wind shear is shown in Fig. 8. Eight different schematics are drawn in Fig. 8 to represent the

placement of the lightning asymmetries in the inner core and outer band regions with different angles between the shear and motion vectors (0°, 90°, 180°, and 270°, each ±45°). The shear vector (**S**) in each diagram is plotted towards the north and the motion vector (**M**) is drawn the appropriate angle counterclockwise from the shear. Locations of expected maxima in lightning associated with vertical wind shear are noted in solid lines and those associated with storm motion in the dashed lines, the same as in Fig. 7.

The quadrant diagrams in Fig. 8 show the number of times the flash count was highest per quadrant for various angles of separation. Over 70% of the time periods studied fall into the top two rows of schematics, the 0° and 90° angle separations, where there is a significant amount of overlap between the motion and shear signatures. In these cases, the shear- and motion-induced lightning maxima coincide in the downshear left quadrant in the inner core and the downshear right quadrant in the outer bands.

In the 0° schematic for the outer bands (top row right of Fig. 8), the shear-related maximum extends into the downshear left quadrant, while the storm motion–related maximum extends into the upshear right quadrant. The shear signature is seen to dominate, with the highest flash counts in the shear-indicated quadrant more than twice as often (13 vs 6) as the motion-indicated quadrant. An even greater dominance of the shear signal is seen in the inner core for the 90° schematic (second row left of Fig. 8) where the shear asymmetry extends to the downshear right quadrant and the motion to the upshear left quadrant. The number of occurrences of highest flash counts in these quadrants was 16 and 3, respectively.

To best evaluate which effect is dominant, time periods where there is little or no overlap between the shear and motion maxima will be examined. In the 180° schematic of Fig. 8 (third row left) the inner core shear and motion maxima are located in opposing quadrants. The highest flash counts favor the shear in 10 of the 13 time periods. In the outer band region (third row right) there is a slight overlap between the shear and motion maxima in the downshear left quadrant, but a clear dominance of the shear signal is seen when the nonoverlapping quadrants are examined. Eighteen time periods had their highest flash count in the downshear right quadrant, while only two were in the right-front quadrant.

Even though the number of cases is quite small with a motion vector 270° left of shear (bottom panels in Fig. 8), the results are similar. In the core, the quadrant of overlap between the shear and motion has the largest number of time periods, but the shear signal wins out with three time periods versus just one for the nonoverlapping quadrants. In the outer band region where there is no overlap between the shear and motion maxima, six of the seven time periods have their highest flash counts downshear of the center and to the left of
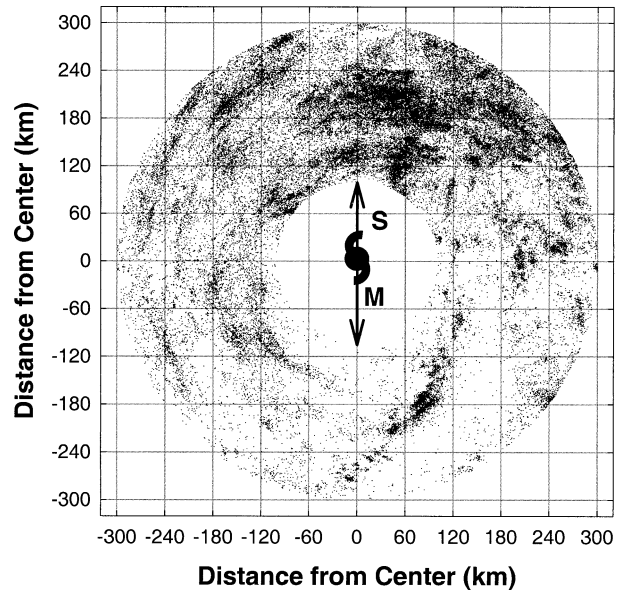

FIG. 9. All flashes in the outer band region of the 33 time periods with an angle of separation between the vertical wind shear and storm motion vectors of 180° ± 45° (corresponds to the third row right panel in Fig. 8). The flashes have been rotated so that the vertical wind shear vector for each time period is pointing due north.

storm motion, indicating the much stronger shear signature once again.

Figure 9 shows all of the lightning flashes that occurred in the outer rainband region in the 33 time periods with a storm motion vector 180° ± 45° to the left of the vertical wind shear vector. The distribution of the speed of motion for these 33 times periods is similar to that for the entire dataset shown in Fig. 2. The plot corresponds with the angle separation in the third row on the right of Fig. 8. Over 77% of the 69 731 flashes are found downshear of the center, with 53% in the downshear-right quadrant. These numbers agree well with the highest flash counts in the outer band quadrant diagram, which also shows a very strong downshear signal.

In the quadrant diagrams, because only the single quadrant with the maximum number of lightning flashes is counted, if the shear signal was dominant but the motion signal was still present we might expect to see a secondary, but smaller, lightning maximum due to storm motion in the right-front quadrant. Figure 9 shows this is not the case, as the minimum number of flashes, 11%, occurs in the right-front quadrant. Also contrary to the motion signature discussed earlier is the left side of the storm having a significantly greater number of flashes than the right-hand side (65% vs 35%). Thus the raw lightning flashes and the quadrant diagrams both support the dominance of the vertical wind shear signal.

6. Discussion

It has been shown that a lightning-based estimate of convective asymmetries with respect to tropical cyclone

motion matches observations made previously using other precipitation-related parameters. The results show a maximum in convection in the front quadrants in the tropical cyclone core ($r < 100$ km) and a right-of-motion maximum in the outer band region.

Corbosiero and Molinari (2002) showed a strong vertical wind shear influence on convective asymmetries as well, with downshear to downshear left maxima in the core and downshear right maxima in the outer bands. Both effects exist only because storm motion is closely coupled to vertical wind shear. Motion is predominantly left of shear (78% of time periods), with more than half of the periods falling between $0°$ and $90°$ left of the shear vector.

To determine whether the vertical wind shear or storm motion effect is dominant, combinations of vertical wind shear and storm motion were chosen that would place the respective convective maxima in opposite quadrants. In these cases, the vertical shear influence showed clearly, while the storm motion influence nearly vanished. The evidence suggests that the well-documented effect of storm motion on convective asymmetries is largely a reflection of the much stronger vertical shear effect.

a. Why is the motion vector left of the shear vector?

Three mechanisms can produce a motion that is left of the vertical wind shear vector:

1) The shear advects the upper-level anticyclone downshear of the center (Wu and Emanuel 1993). Regardless of the direction of shear, this process induces flow perpendicular and to the left of the shear vector, and thus by itself introduces a leftward deflection of the motion from the shear.
2) The beta effect by itself induces northwestward motion. This motion is left of shear for all shear values from the southwest half of the circulation [i.e., shear having meteorological directions from southeast ($135°$) counterclockwise to northwest ($315°$)]. This range includes the dominant southwest-to-west vertical shear directions in this study. In contrast, the beta effect produces right-of-shear storm motion for shear vectors coming from the northeast half of the circulation.
3) A nonzero second derivative of the zonal wind with height is associated with a meridional potential vorticity gradient that conceptually acts the same as the beta effect. If the second derivative is negative (increasing easterly shear or decreasing westerly shear with height), it will require a poleward potential vorticity gradient and thus a left-of-shear deflection if the shear has a component from the west.

The first effect in this list holds for all directions of shear and is thus a possible factor. It is least likely to be important when shear is small and the resultant downshear shift of the upper anticyclone is small. The latter

hypothesis is supported: 37% of weak shear periods contain motion right of shear, while only 15% of moderate- or strong-shear time periods do so. The predominance of motion left of shear, and its enhancement when shear is moderate or strong, each support the downshear tilt of the anticyclone as having a significant impact.

If the beta effect is important, the percentage of storms with motion left of shear should be larger when the shear is between $135°$ and $315°$ than when it is between $315°$ and $135°$. This is borne out: 82% of the periods with shear from the southwest half move left of shear, versus 58% from the northeast half. The beta effect is more clearly isolated if only weak-shear time periods are considered, because then the downshear anticyclone influence is minimized. Under these circumstances, more than 75% of storms move left of shear in the southwest half, and more than 75% move right of shear in the northeast half. The latter examples show that the beta effect overcomes the outflow anticyclone effect when shear is weak, confirming that beta can play a significant role.

With regard to the third effect in the list, a vertical profile of the zonal wind averaged over westerly shear time periods (not shown) shows a nearly constant westerly shear with height above the boundary layer, and thus a small second derivative. This holds for mean profiles of time periods with motion both left and right of shear, suggesting that, in the mean, the nonlinear shear is having little impact. Overall, the evidence indicates that the tilt of the upper anticyclone dominates the shear–motion relationship in tropical cyclones when shear is moderate or strong, and the beta effect becomes important when the shear is weak.

Finally, it should be noted that if the *cyclonic* portion of the vortex tilted downshear with height, it would induce motion to the *right* of the shear (Dengler and Reeder 1997; Jones 1995). Because the latter so rarely occurs, it implies that vertical tilt may be small in the cyclonic part of the vortex. This supports the same arguments made by Corbosiero and Molinari (2002) based on the distribution of convection with respect to the shear vector. It is argued that deep convection acts to keep the tropical cyclone nearly upright in the cyclonic part of the vortex, but this effect does not substantially reach the layer of the outflow anticyclone. Rather, the latter frequently is carried downshear, contributing to the common left-of-shear motion of tropical cyclones.

Few observations of hurricane tilt exist to confirm or refute the above hypothesis. Reasor et al. (2000) report tilts in Hurricane Olivia (1994) ranging from nearly 0 to 8 km in the cyclonic part of the vortex, depending on the magnitude of the shear. In a high-resolution numerical model simulation, Rogers et al. (2002, manuscript submitted to *Mon. Wea. Rev.*) found tilts of 7–14 km in Hurricane Bonnie (1998). It seems likely that tilts on the high end of these values would increase the likelihood that the storm motion vector would lie to the right of the shear vector, yet such a configuration is

rarely seen in this study. It is possible that significant tilt of the storm core is transient and does not influence the motion on the 12-h timescales used in this paper. This paradox can only be resolved by more observations of tilt and its time change in real storms.

b. Why does the asymmetric friction effect not show in the convection?

Given that the dynamics of asymmetric friction are well understood in theory (Shapiro 1983), it must be asked why the effects do not seem to appear in nature. Two possible influences play a role. First, in a sheared environment the mean current (i.e., with the vortex removed) in the planetary boundary layer is almost always much less than the mean cross-storm current in the upper troposphere. As a result, the mean current in the boundary layer can be considerably less than the storm motion. In Shapiro's integrations, which were confined to a slab boundary layer, the two were assumed to be equal. The asymmetric frictional forcing would be overestimated by that assumption. These arguments are supported by a profile of mean wind speed for the 20 fastest-moving time periods in this study. The mean boundary layer wind was 4.5 m s^{-1}, the mean speed of storm motion was 8.3 m s^{-1}, and the mean upper-tropospheric wind speed was 12 m s^{-1}. The asymmetries in friction would clearly be smaller than if a basic current equal to the mean storm motion had been added to the boundary layer flow.

Second, Shapiro's calculations only predict the vertical motion at the top of the boundary layer. If vertical wind shear acts to produce deep subsidence in the front and right-front quadrants, asymmetric friction might produce only a shallow upward motion that does not result in convection owing to free-atmosphere stabilization by the shear-induced circulation. Some support for this argument comes from the literature. Reasor et al. (2000) noted that the storm motion in Hurricane Olivia (1994) was nearly constant while the pattern of vertical velocity became highly asymmetric in time. They attributed this to an increase in the magnitude of the vertical wind shear from 3 to 15 m s^{-1} in just 2.5 h. Frank and Ritchie (1999) show numerical integrations in which shallow upward motion without convection occurs in the front and right-front quadrants. Strong convection occurs in these integrations in the downshear left quadrant where shear influences are large. Finally, Bender (1997) shows an integration on a beta plane with no external shear. In that integration, the beta gyre–induced shear gives convection downshear and no convection in the front or right-front quadrants. In all of these examples, the shear effect dominated the asymmetric friction effect, even when shear was as small as 3–4 m s^{-1}. Overall, based on the results of this study and those studies referred to earlier, it is argued that the asymmetric frictional effect that shows so clearly in the literature (Fig. 1) and in the results of this paper (Figs.

3 and 4) is in fact largely a reflection of the much stronger vertical wind shear influences on convective asymmetries. The influence of asymmetric friction is real, but apparently it has little impact on convective asymmetries unless vertical wind shear is negligible.

REFERENCES

Bender, M. A., 1997: The effect of relative flow on the asymmetric structure of the interior of hurricanes. *J. Atmos. Sci.,* **54,** 703–724.

Black, M. L., R. W. Burpee, and F. D. Marks Jr., 1997: The asymmetric distribution of vertical motions and precipitation in the hurricane eyewall. Preprints, *22d Conf. on Hurricanes and Tropical Meteorology,* Fort Collins, CO, Amer. Meteor. Soc., 100–101.

Burpee, R. W., and M. L. Black, 1989: Temporal and spatial variations of rainfall near the centers of two tropical cyclones. *Mon. Wea. Rev.,* **117,** 2204–2218.

Chan, J. C. L., and W. M. Gray, 1982: Tropical cyclone movement and surrounding flow relationships. *Mon. Wea. Rev.,* **110,** 1354–1374.

Cline, I. M., 1926: *Tropical Cyclones.* MacMillan, 301 pp.

Corbosiero, K. L., and J. Molinari, 2002: The effects of vertical wind shear on the distribution of convection in tropical cyclones. *Mon. Wea. Rev.,* **130,** 2110–2123.

Dengler, K., and M. J. Reeder, 1997: The effects of convection and baroclinicity on the motion of tropical cyclone like vortices. *Quart. J. Roy. Meteor. Soc.,* **123,** 699–725.

Fiorino, M., and R. L. Elsberry, 1989: Some aspects of vortex structure related to tropical cyclone motion. *J. Atmos. Sci.,* **46,** 975–990.

Flatau, M., W. H. Schubert, and D. E. Stevens, 1994: The role of baroclinic processes in tropical cyclone motion: The influence of vertical tilt. *J. Atmos. Sci.,* **51,** 2589–2601.

Frank, W. M., 1977: The structure and energetics of the tropical cyclone. I. Storm structure. *Mon. Wea. Rev.,* **105,** 1119–1135.

——, and E. A. Ritchie, 1999: Effects of environmental flow upon tropical cyclone structure. *Mon. Wea. Rev.,* **127,** 2044–2061.

Franklin, J. L., S. J. Ford, S. E. Feuer, and F. D. Marks Jr., 1993: The kinematic structure of Hurricane Gloria (1985) determined from nested analyses of dropwindsonde and Doppler radar data. *Mon. Wea. Rev.,* **121,** 2433–2451.

——, S. E. Feuer, J. Kaplan, and S. D. Aberson, 1996: Tropical cyclone motion and surrounding flow relationships: Searching for beta gyres in Omega dropwindsonde data sets. *Mon. Wea. Rev.,* **124,** 64–84.

Gamache, J. F., H. E. Willoughby, M. L. Black, and C. E. Samsury, 1997: Wind shear, sea surface temperature and convection in hurricanes observed by airborne Doppler radar. Preprints, *22d*

Conf. on Hurricanes and Tropical Meteorology, Fort Collins, CO, Amer. Meteor. Soc., 121–122.

Jones, S. C., 1995: The evolution of vortices in vertical shear. I: Initially barotropic vortices. *Quart. J. Roy. Meteor. Soc.,* **121,** 821–851.

Jorgensen, D. P., E. J. Zipser, and M. A. LeMone, 1985: Vertical motions in intense hurricanes. *J. Atmos. Sci.,* **42,** 839–856.

Marks, F. D., Jr., 1985: Evolution of the structure of precipitation in Hurricane Allen (1980). *Mon. Wea. Rev.,* **113,** 909–930.

——, R. A. Houze Jr., and J. F. Gamache, 1992: Dual-aircraft investigation of the inner core of Hurricane Norbert. Part I: Kinematic structure. *J. Atmos. Sci.,* **49,** 919–942.

Miller, B. I., 1958: Rainfall rates in Florida hurricanes. *Mon. Wea. Rev.,* **86,** 258–264.

Molinari, J., S. Skubis, and D. Vollaro, 1995: External influences on hurricane intensity. Part III: Potential vorticity structure. *J. Atmos. Sci.,* **52,** 3593–3606.

——, ——, ——, F. Alsheimer, and H. E. Willoughby, 1998: Potential vorticity analysis of tropical cyclones intensification. *J. Atmos. Sci.,* **55,** 2632–2644.

——, P. Moore, and V. Idone, 1999: Convective structure of hurricanes as revealed by lightning locations. *Mon. Wea. Rev.,* **127,** 520–534.

Parrish, J. R., R. W. Burpee, F. D. Marks Jr., and R. Grebe, 1982: Rainfall pattern observed by digitized radar during the landfall of Hurricane Frederic (1979). *Mon. Wea. Rev.,* **110,** 1933–1944.

Reasor, P. D., M. T. Montgomery, F. D. Marks Jr., and J. F. Gamache, 2000: Low-wavenumber structure and evolution of the hurricane inner core observed by airborne dual-doppler radar. *Mon. Wea. Rev.,* **128,** 1653–1680.

Rodgers, E. B., S. W. Chung, and H. F. Pierce, 1994: A satellite observational and numerical study of precipitation characteristics in western North Atlantic tropical cyclones. *J. Appl. Meteor.,* **33,** 129–139.

Shapiro, L. J., 1983: Asymmetric boundary layer flow under a translating hurricane. *J. Atmos. Sci.,* **40,** 1984–1998.

——, 1992: Hurricane vortex motion and evolution in a three-layer model. *J. Atmos. Sci.,* **49,** 140–153.

Wang, Y., and G. J. Holland, 1996: Tropical cyclone motion and evolution in vertical shear. *J. Atmos. Sci.,* **53,** 3313–3332.

Willoughby, H. E., F. D. Marks Jr., and R. J. Feinberg, 1984: Stationary and moving convective bands in hurricanes. *J. Atmos. Sci.,* **41,** 3189–3211.

Wu, C.-C., and K. A. Emanuel, 1993: Interaction of a baroclinic vortex with background shear: Application to hurricane movement. *J. Atmos. Sci.,* **50,** 62–76.

——, and ——, 1995a: Potential vorticity diagnostics of hurricane movement. Part I: A case study of Hurricane Bob (1991). *Mon. Wea. Rev.,* **123,** 69–92.

——, and ——, 1995b: Potential vorticity diagnostics of hurricane movement. Part II: Tropical Storm Ana (1991) and Hurricane Andrew (1992). *Mon. Wea. Rev.,* **123,** 93–109.